Journal of Power Sources 194 (2009) 746–752

Contents lists available at ScienceDirect

Journal of Power Sources

journal homepage: www.elsevier.com/locate/jpowsour

Molecular structure and transport dynamics in Nafion and sulfonated poly(ether ether ketone ketone) membranes

P.Y. Chen, C.P. Chiu, C.W. Hong*

Department of Power Mechanical Engineering, National Tsing Hua University, 101, Sec. 2, Kwang Fu Road, Hsinchu 30013, Taiwan

ARTICLE INFO

Article history:
Received 9 April 2009
Received in revised form 26 May 2009
Accepted 3 June 2009
Available online 11 June 2009

Keywords:
Molecular simulation
Sulfonated poly(ether ether ketone ketone) (SPEEKK)
Methanol permeation

ABSTRACT

An atomistic simulation technique is performed to investigate the molecular structure and transport dynamics inside a hydrated Nafion membrane and a hydrated sulfonated poly(ether ether ketone ketone) (SPEEKK) membrane. The simulation system consists of the representative fragments of the polymer electrolytes, hydronium ions and solvent molecules, such as water plus methanol molecules. Simulation results show that the hydrated SPEEKK has less phase separation among hydrophobic and hydrophilic regions in comparison with the Nafion. Those water channels formed in the SPEEKK are much narrower compared to those in the Nafion. These characteristics lead to a lower mobility of hydronium ions and water molecules and hence relatively lower diffusion coefficient of methanol in the SPEEKK. It results in the reduction of the methanol permeation problem in direct methanol fuel cells.

1. Introduction

Polymer electrolyte based fuel cells, including proton exchange membrane fuel cells (PEMFCs) and direct methanol fuel cells (DMFCs), are considered as the most promising power sources for portable electronic devices and future clean vehicles [1]. Currently, Nafion membranes manufactured by Dupont are the most popular electrolytes used in PEMFCs and DMFCs. This is because of the acceptable proton conductivity as well as high chemical and mechanical stabilities. However, high cost and serious methanol permeation have limited Nafion and other similar perfluorinated membranes for commercial application in DMFCs. Over the past decade, there were many studies to develop non-perfluorinated polymers as the alternative membranes, such as sulfonated poly(aryl ether ketone)s, sulfonated polysulfones, sulfonated polybenzimidazoles, sulfonated polyimides and some others [2]. Sulfonated poly(ether ether ketone ketone) (SPEEKK) is a member of the sulfonated poly(aryl ether ketone) family and is regarded as a potential candidate for future solid electrolyte espectially in DMFCs [3].

Some experimental studies have also been carried out to understand the microstructure and the ionic transport inside the SPEEKK membrane. For example, atomic force microscopy (AFM) and scanning electron microscope (SEM) methods were used to investigate the surface morphology of the SPEEKK membrane [4,5]. Electrophoretic nuclear magnetic resonance (ENMR) was applied to measure the electro-osmotic drag coefficients in Nafion and SPEEKK membranes [6]. The states of ionic aggregations were observed by using transmission electron microscope (TEM), small angle X-ray scattering (SAXS), Fourier transform infrared (FTIR) techniques and etc. [7–9]. In contrast to several experimental literatures reported above, only few theoretical investigations have been presented. Paddison performed *ab initio* molecular orbital calculations to investigate the proton dissociation in the hydrophilic parts of hydrated Nafion and SPEEKK membranes [10]; the proton transport phenomenon within the membrane pores were studied. Using a molecular structure-function modeling method, the same author computed the proton friction and diffusion coefficients inside the SPEEKK membrane at various levels of hydration [11]. However, the membrane morphology and the distribution of water clusters in the SPEEKK membrane have not been explored in the previous investigations. This paper intends to further investigate and to compare the molecular structure and transport dynamics of hydrated Nafion and SPEEKK membranes by means of molecular dynamics technique; which is an extension to our previous research [12,13]. The morphology difference between hydrated Nafion and SPEEKK membranes will be visualized from our simulation results. Methanol permeability in these two membranes will also be investigated. Details of molecular modeling and simulation techniques are described in the following section.

* Corresponding author. Tel.: +886 3 5742591; fax: +886 3 5722840.
E-mail address: cwhong@pme.nthu.edu.tw (C.W. Hong).

0378-7753/$ – see front matter © 2009 Elsevier B.V. All rights reserved.
doi:10.1016/j.jpowsour.2009.06.011

Nomenclature

A	parameters for dihedral potential function (kcal mol^{-1})
a	parameters for 12-6 potential function (Å^{12})
b	parameters for 12-6 potential function (Å^{6})
D	diffusion coefficient (Å^2 ps^{-1})
KE	kinetic energy (kcal mol^{-1})
k_a	force constants for valence angle potential function (kcal mol^{-1} rad^{-2})
k_b	force constants for bond potential function (kcal mol^{-1} Å^{-2})
m	parameters for dihedral potential function
N	number of atoms
r_{ij}	distance between atom i and atom j (Å)
$\vec{r}_n$	position vectors (Å)
r_0	equilibrium bond length (Å)
t	time (ps)
U	potential energies (kcal mol^{-1})
V	volume (Å^3)
δ	parameters for dihedral potential function (deg)
θ	instant valence angle (rad)
θ_0	equilibrium valence angle (rad)
ρ	number density (Å^{-3})
ϕ	instant torsion angle (deg)

2. Molecular modeling and computer simulation

2.1. Molecular modeling

The molecular simulation system mainly consists of the polymer electrolyte (case 1 is the Nafion and case 2 is the SPEEKK fragments), hydronium ions, and solvent molecules, such as pure water or water plus methanol molecules. Fig. 1 shows the chemical structure of the Nafion and the SPEEKK membrane. For simplification in molecular dynamics, the realistic membrane was represented by fragments of the chemical structure instead of the complete compositions. The long backbone of the Nafion (and the SPEEKK) membrane is repeated and can be truncated; the pendant side chain attached to the main backbone is maintained to avoid affecting the original characteristics. Fig. 2 shows the simplified Nafion and SPEEKK fragments in the simulation; the initial conformation for each fragment was constructed by a semi-empirical charge distribution method (Austin Model 1) using quantum chemical calculation [14]. The calculation was considered to be converged when the gradient of the atomic force was less than the preset value (0.01 kcal mol^{-1} Å^{-1} in our case). Once convergence was attained, an optimal geometry of the fragment was constructed and the distribution of charges was assigned.

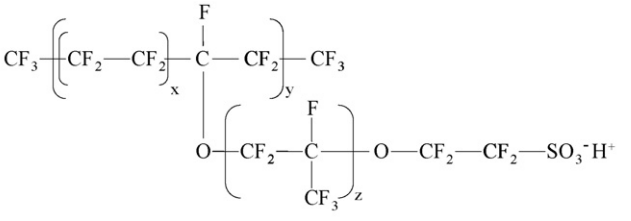

(a) Nafion (x=5-10, $y \approx 1000$ and z=1-2)

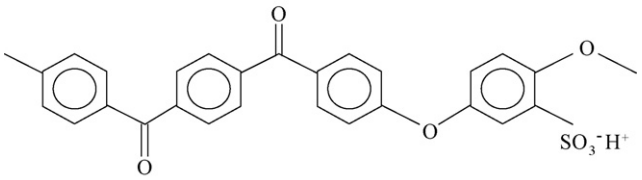

(b) SPEEKK

Fig. 1. Chemical structure of (a) the Nafion and (b) the SPEEKK membrane.

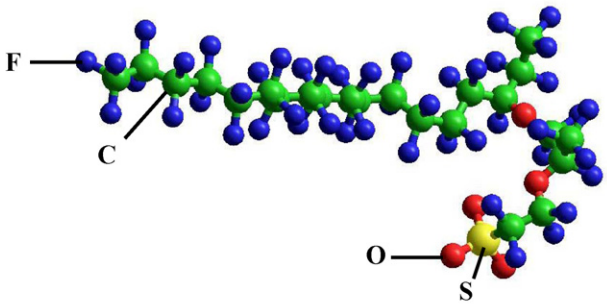

(a) Nafion

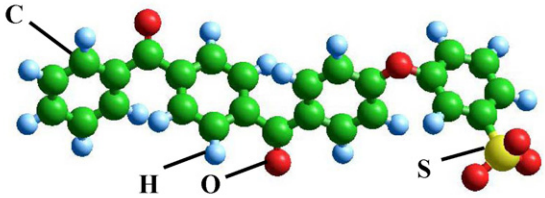

(b) SPEEKK

Fig. 2. Simplified molecular structure of (a) Nafion and (b) SPEEKK fragments in the simulation (F: fluorine in deep blue; C: carbon in green; H: hydrogen in light blue; S: sulfur in yellow; O: oxygen in red). (For interpretation of the references to color in this figure legend, the reader is referred to the web version of the article.)

Each proton that migrates inside the electrolyte is assumed to form a hydronium ion (H_3O^+) with one water molecule. The hydronium ion is the simplest type of an oxonium ion, which migrates towards the cathode by the vehicle and the Grotthuss mechanisms [15]. To achieve electrical neutrality, the number of H_3O^+ is assigned to equal the number of sulfonic-acid (SO_3^-) groups. Table 1 summarizes the simulation conditions of the investigated system. We chose those cases of water uptakes according to the experimental conditions in Ref. [9]. The definition of water uptake is the total weight of water divided by the weight of the dry membrane in experiment; however, in the simulation we transform them into the ratio of the number of molecules. The number of water molecules in the Nafion is set to be same as that in the SPEEKK; and the total number of water and methanol molecules is fixed (186 in our case). This was to test the methanol permeability at different methanol concentration in the later case in Table 2. Water and methanol molecules are initially assigned to distribute randomly inside the simulation system.

Table 1
Summary of simulation conditions.

	Membrane			
	Nafion		SPEEKK	
Water uptake (%)	10.00	9.08	16.00	14.53
No. of fragments	32	32	32	32
No. of hydronium ions	32	32	32	32
No. of water molecules	186	166	186	166
No. of methanol molecules	0	20	0	20

Water uptake (%) $= \frac{\text{total weight of water molecules}}{\text{weight of dry membrane}} \times 100$.

Table 2
Density and volume of the MD simulation system obtained from the 1.5-ns NPT simulation.

	Membrane			
	Nafion		SPEEKK	
Weight percentage wt% (CH_3OH)	0	15.11	0	15.11
Molar concentration M (CH_3OH)	0	4.56	0	4.56
Density ($g\,cm^{-3}$)	1.83	1.76	1.21	1.17
Volume ($Å^3$)	$(34.0)^3$	$(34.5)^3$	$(59.3)^3$	$(60.0)^3$

$\text{wt\% } (CH_3OH) = \frac{\text{total weight of } CH_3OH}{\text{total weight of } CH_3OH, H_2O \text{ and } H_3O^+}$.
$\text{M } (CH_3OH) = \frac{\text{mole of } CH_3OH}{\text{total volume of } CH_3OH, H_2O \text{ and } H_3O^+}$.

2.2. Computer simulation

In the Hamiltonian system, the total energy is expressed by:

$$U_{total} = U_{inter} + U_{intra} + KE \quad (1)$$

where U_{total} is the total energy, U_{inter} is the inter-molecular potential energy, U_{intra} is the intra-molecular potential energy, and KE is the kinetic energy. The inter-molecular potential includes the van der Waals potential and the electrostatic potential. The van der Waals force was expressed by the typical 12-6 Lennard–Jones function. For multi-atom molecules, the intra-molecular potential includes the valence angle potential (U_{angle}), the bond potential (U_{bond}), and the dihedral angle potential ($U_{dihedral}$). These potential functions are expressed by:

$$U_{angle}(\theta) = \frac{k_a}{2}(\cos\,\theta - \cos\theta_0)^2 \quad (2)$$

$$U_{bond}(r_{ij}) = \frac{k_b}{2}(r_{ij} - r_0)^2 \quad (3)$$

$$U_{dihedral}(\phi) = A[1 + \cos(m\phi - \delta)] \quad (4)$$

where k_a, k_b are force parameters of the angle and the bond potentials; A, m and δ are parameters in the dihedral potential function; θ and ϕ are the bond and the torsion angles. These parameters were evaluated from the DREIDING force field developed by Mayo et al. [16]. For methanol molecule, the three-site potential model [17] was employed. The force parameters of the O–H and O–CH_3 stretching and CH_3–O–H bending were obtained from the all-atom force fields [18]. The rigid three-site SPC/E model [19] was adopted for water molecules and the force-field parameters of the hydronium ion were obtained from the classical force fields presented by Burykin and Warshel [20].

Molecular dynamics (MD) simulation was carried out on an IBM P690 workstation using the software DLPOLY [21]. A period of 1.5-ns NPT (constant number of particles, constant pressure and constant

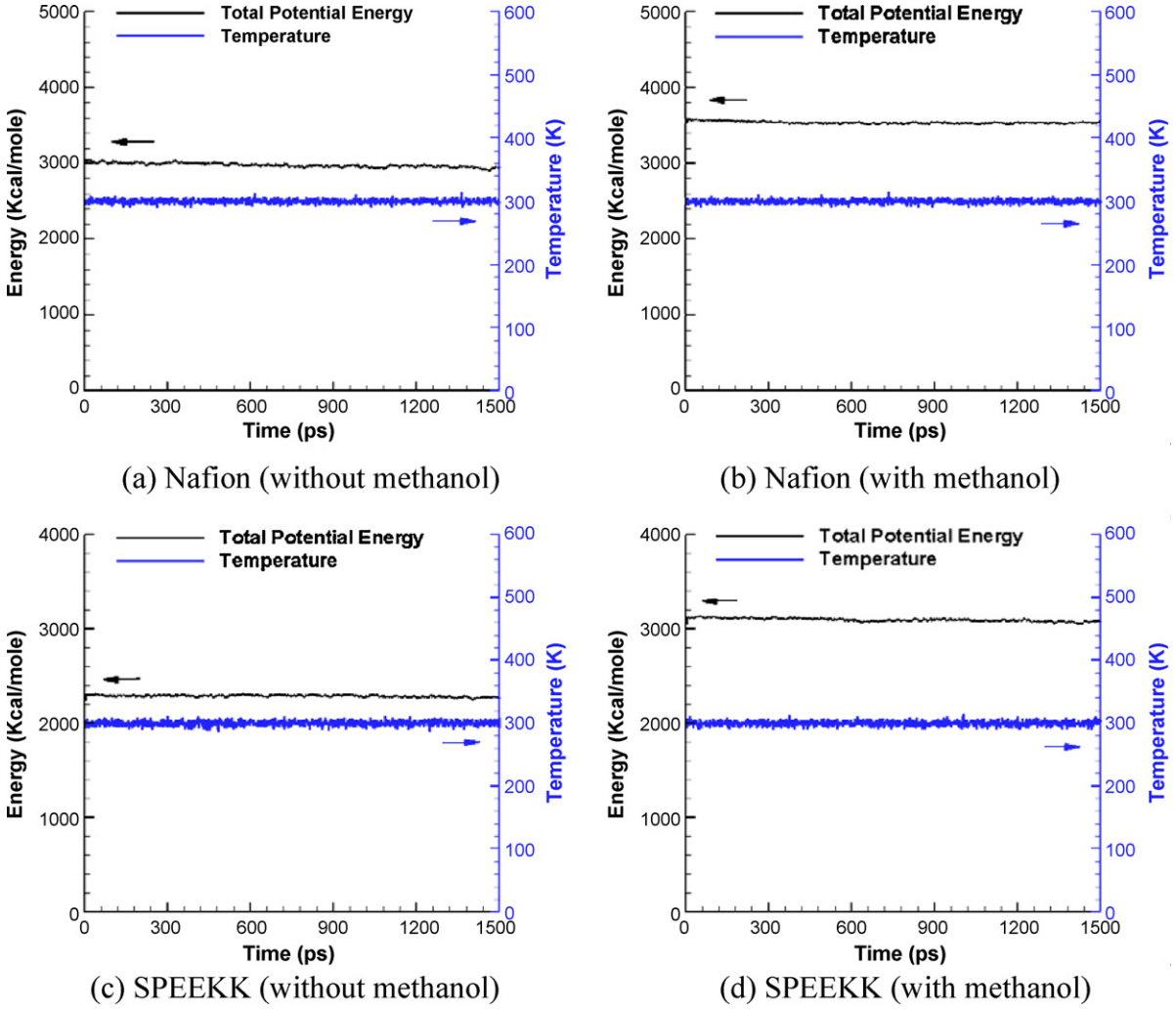

Fig. 3. Total energy and temperature variation of the MD simulation system for (a) Nafion without methanol, (b) Nafion with methanol, (c) SPEEKK without methanol and (d) SPEEKK with methanol (all at 300 K).

temperature) ensemble simulation was performed to tune the simulation system to reach a proper density. It was followed by another 1.5-ns NVT (constant number of particles, constant volume and constant temperature) simulation. All MD simulations were performed at 300 K (27 °C) and the equations of motion were solved with a Verlet scheme [22] with a time step 1 fs. The Lennard–Jones and electrostatic potentials were truncated at 10 Å. All covalent bonds were kept rigid with the SHAKE algorithm [23] and three-dimensional periodic boundary conditions were applied in the simulation. The Eward summation method [24] was used for the calculation of the electrostatic potential at the periodic boundary condition.

3. Results and discussion

3.1. System equilibrium

Table 2 shows the calculated density and volume of the equilibrated system obtained from the preliminary 1.5-ns NPT simulation. This was to emulate the membrane swelling with uptake of methanol. The weight percentage of methanol is calculated as the ratio between the total weight of methanol molecules and the total weight of methanol plus water molecules plus hydronium ions. The molar concentration of methanol is defined as the number of moles of methanol divided by the total volume of methanol plus water molecules plus hydronium ions. The total volume is evaluated from the NPT simulation based on the input from Table 1. Before analyzing the simulation results, we checked the equilibration of the system by monitoring the total energy and the temperature variation during the formal 1.5-ns NVT simulation. Fig. 3 shows that both total potential energy and temperature are converged in each simulation case. Fluctuations in the total energy output are less than ±5%, which are caused by the exchange of the potential and the kinetic energy. Checking from the detailed data, the electrostatic potential contributes more than 50% of the total energy, implying that the influence from the Coulombic force is the most significant; while the influence from the dihedral potential is the least.

3.2. Membrane morphology analysis

The ion conduction properties of the membrane closely relate to the internal structure such as the spatial distribution of ionic sites in the membrane. The snapshots of the membrane morphology from the MD simulation can be seen in Fig. 4(a)-Nafion and (b)-SPEEKK. Both hydrated Nafion and SPEEKK membranes form the phase separation of hydrophobic and hydrophilic parts. Our simulation results show a good agreement with the experimental observation from the Ref. [25]. The hydrophobic region is constituted by the backbone (green cloud) of the polymer, while the hydrophilic region contains water molecules (gray cloud), hydronium ions (light blue balls) and sulfonic-acid groups (yellow and red balls). In comparison with the hydrated Nafion in Fig. 4(a), the hydrated SPEEKK in Fig. 4(b) forms less hydrophobic/hydrophilic phase separations. The water channels in the Nafion are approximately 1–3 nm in diameter while those in the SPEEKK are approximately 0.5–1 nm. The nanoscopic simulation reveals that the water channels in the SPEEKK are narrower and less in quantity than those in the Nafion. These features show a larger interface between the hydrophobic and hydrophilic regions in the SPEEKK; implying that the average distance between the neighboring sulfonic-acid groups in the SPEEKK is larger than that in the Nafion membrane.

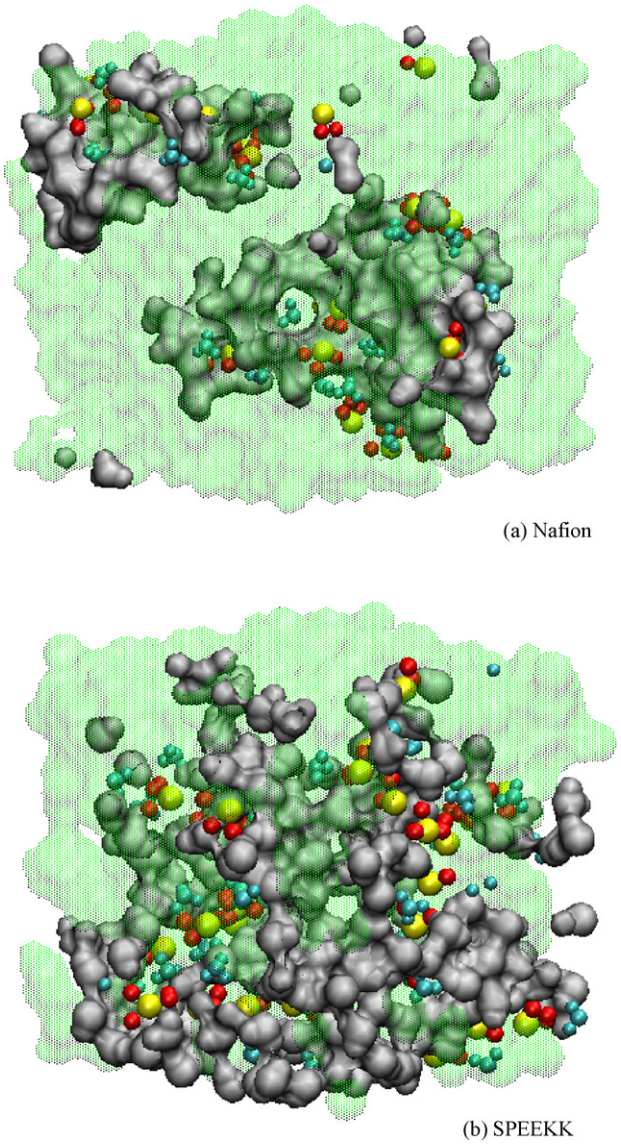

Fig. 4. Snapshots of the membrane morphology from the MD simulation for (a) Nafion and (b) SPEEKK membranes (light blue balls: hydroniums; red balls: oxygen atoms; yellow balls: sulfur atoms; gray cloud: water molecules; green cloud: backbones of the polymer). (For interpretation of the references to color in this figure legend, the reader is referred to the web version of the article.)

3.3. Molecular structure analysis

The radial distribution function (RDF), denoted as $g(r)$, is an indication of the local molecular structure and is defined mathematically by

$$g(r) = \frac{\langle N(r, \Delta r)\rangle}{(1/2)N\rho V(r, \Delta r)} = \frac{\rho(r)}{\rho} = \frac{\text{local number density}}{\text{system number density}} \quad (5)$$

where $\langle\ \rangle$ indicates a temporal average; $N(r, \Delta r)$ is the number of atoms within the spherical shell of radius between r and $r+\Delta r$; N is the total number of atoms in the system; ρ is the number density and $V(r, \Delta r)$ is the volume of the shell. Fig. 5(a) shows the RDFs of molecule pairs of the carbon-water (in which water is represented by the oxygen atom in it) and the fluorine-water for the Nafion membrane; there the RDFs increase almost with the radius and the height of RDFs is less than unity, implying that these two atoms, F and C, are hydrophobic during the simulation period. The RDF variation tendency observed in Fig. 5(b), RDFs of molecule pairs

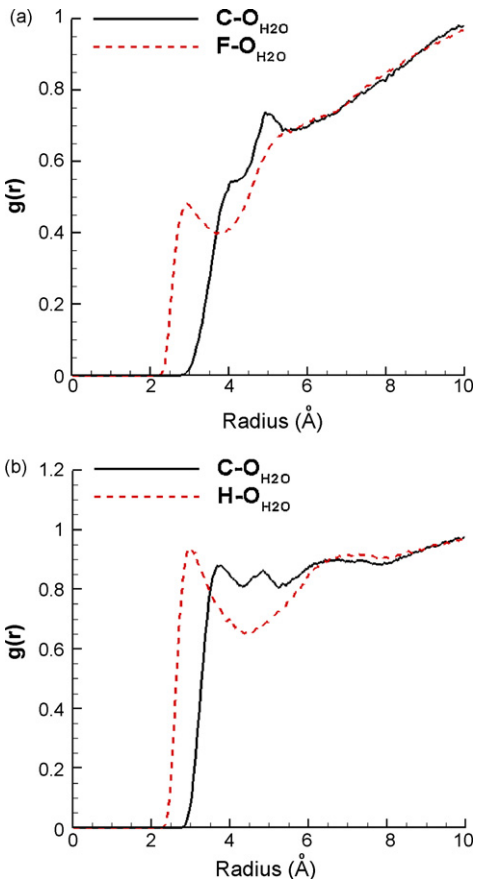

Fig. 5. RDFs of (a) C–O_{H_2O}, F–O_{H_2O} pairs for Nafion and (b) C–O_{H_2O}, H–O_{H_2O} pairs for SPEEKK at 300 K.

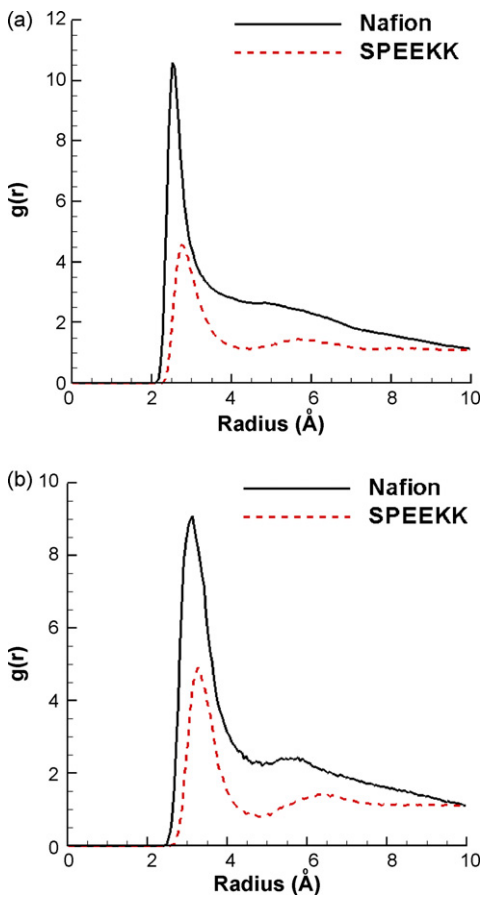

Fig. 7. RDFs of (a) O_{H_2O}–O_{H_2O} and (b) O_{H_2O}–$O_{H_3O^+}$ pairs for Nafion and SPEEKK membranes at 300 K.

of carbon-water and hydrogen-water for the SPEEKK membrane, reveals that both carbon and hydrogen atoms are hydrophobic due to RDFs stay around 0.8 after 2.8 Å and 3.8 Å, respectively. The RDFs of oxygen atoms (denoted as Os) in the sulfonic-acid groups toward water molecules for the Nafion and the SPEEKK are shown in Fig. 6. First peaks are observed at the radius about 2.5 Å for the Nafion and 2.75 Å for the SPEEKK, which indicate that water molecules tend to aggregate near the sulfonic-acid groups in both membranes. Molecules staying at the first peak of the RDF diagram correspond to the "bound state" and are restrained from moving freely. In addition, the height of the first peak of the Nafion is greater than that of the SPEEKK, implying that the local number density of water molecules associated with the sulfonic-acid groups in the Nafion is greater than that in the SPEEKK. Fig. 7(a) and (b) shows the RDFs of molecule pairs of water-water and water-hydronium for the Nafion and the SPEEKK membranes. Significant first peaks in both (a) and (b) indicate that water molecules tend to form clusters and they can drag the hydronium ions to travel in these two membranes. The dragging effect is less significant in the SPEEKK than in the Nafion.

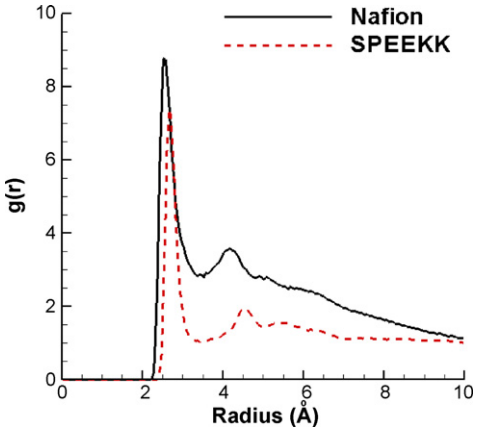

Fig. 6. RDFs of Os–O_{H_2O} pair for Nafion and SPEEKK membranes at 300 K.

Fig. 8 shows the distributions of water clusters and their sizes in the Nafion and the SPEEKK membranes. Water molecules are assumed to belong to the same cluster if the distance between the oxygen atoms from different water molecules is less than 3.5 Å. It is shown that water molecules in the SPEEKK form more clusters in comparison with the Nafion, 54 versus 58 as indicated by the arrows in the diagram; while the average size of water clusters in the SPEEKK is smaller than that in the Nafion. Water molecules are considered to form a hydrophilic aggregation with the sulfonic-acid groups when the distance between the oxygen atom of the RSO_3^- and the oxygen atom of the water is within a preset value (2.5 Å for the Nafion and 2.75 Å for the SPEEKK, respectively). The chosen value corresponds to the average distance of the first hydration shell around the sulfonic-acid groups. The average numbers of water molecules around a specific sulfonic-acid group are 4.35 for the Nafion and 3.07 for the SPEEKK. The results of water clusters distributions and hydrophilic aggregations analysis agree well with the membrane morphology shown in Fig. 4, where the hydrated Nafion forms a larger hydrophobic/hydrophilic phase separation and the water channels in the Nafion are wider than those in the SPEEKK. These features lead to a rise in the size of water clusters and the hydrophilic aggregation in the Nafion than in the SPEEKK membrane.

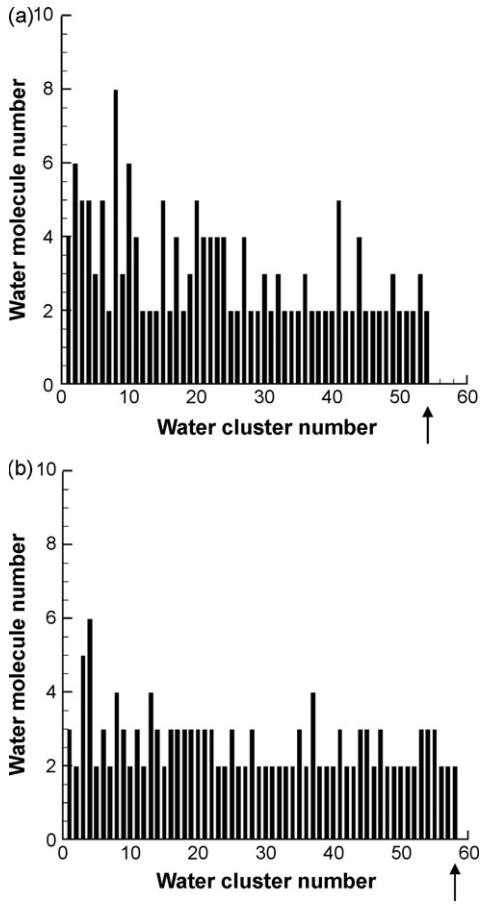

Fig. 8. Distribution of water molecule number versus water cluster number inside (a) Nafion and (b) SPEEKK membranes.

3.4. Molecular mobility analysis

The mobility of molecules can be analyzed using the mean square displacement (MSD), which is defined mathematically by:

$$\mathrm{MSD} = \frac{1}{N}\sum_{n=1}^{N}\left\langle [\vec{r_n}(t_0+t) - \vec{r_n}(t_0)]^2 \right\rangle \quad (6)$$

where N is the number of molecules; $\vec{r}_n(t)$ is the position vector of molecule n at time t and t_0 is the initial time step. Fig. 9 shows the MSDs of hydronium ions and water molecules for the Nafion and the SPEEKK membranes. Linear tendencies of the MSD curves infer that the hydronium ions and water molecules are diffusing continuously in the system during the simulation. Both hydronium ions and water molecules show a greater slope of MSD curves in the Nafion than in the SPEEKK. Diffusion coefficients can be evaluated from the Einstein relation as below

$$D = \frac{1}{6N}\lim_{t\to\infty}\frac{d}{dt}\sum_{n=1}^{N}\left\langle [\vec{r_n}(t_0+t) - \vec{r_n}(t_0)^2 \right\rangle \quad (7)$$

where D is the diffusion coefficient, N is the number of molecules or ions, and $\vec{r}_n(t)$ is the position vector of molecule or ion n at time t. Table 3 shows the comparison of diffusion coefficients of water molecules in the Nafion and the SPEEKK between simulations and experiments. Our predictions are in reasonable agreement with the experimental results from Refs. [9] and [12] (0.42×10^{-5} cm^2 s^{-1} for the Nafion and 0.30×10^{-5} cm^2 s^{-1} for the SPEEKK, respectively). MD predictions of the ionic conductivity of hydronium ions in the Nafion and in the SPEEKK membranes are 0.011 S cm^{-1} and 0.003 S cm^{-1}, respectively. They are about one third of the experimental results reported from Refs. [8,26] as shown in Table 4. The discrepancy comes from the molecular model that we only consider the vehicle mechanism for modeling the hydronium transport; while the transfer of proton hopping (i.e., the Grotthuss mechanism) between hydronium ions and water molecules is not included. The later mechanism needs more detailed quantum simulation. Summarily, the mobilities of hydronium ions and water molecules in the SPEEKK are lower than those in the Nafion. This can be explained by the narrower water channels and less hydrophilic aggregations in the SPEEKK restrict the migration of hydronium ions and water molecules.

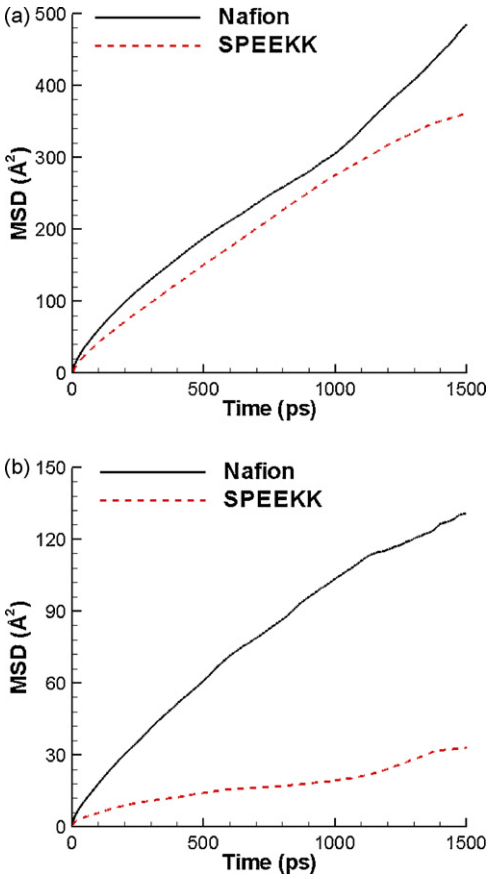

Fig. 9. MSDs of (a) water molecules and (b) hydronium ions for Nafion and SPEEKK membranes at 300 K.

Table 3
Comparison of diffusion coefficient of water molecules in the Nafion and the SPEEKK between simulation results and similar experiments [9,12].

Diffusion coefficient (cm^2 s^{-1}) of water molecules	Membrane	
	Nafion	SPEEKK
MD prediction	0.55×10^{-5}	0.39×10^{-5}
Experiment	0.42×10^{-5}	0.30×10^{-5}

Table 4
Comparison of ionic conductivity of hydronium ions in the Nafion and the SPEEKK between simulation results and similar experiments [8,26].

Ionic conductivity (S cm^{-1}) of hydronium ions	Membrane	
	Nafion	SPEEKK
MD prediction	0.011	0.003
Experiment	0.038	0.013

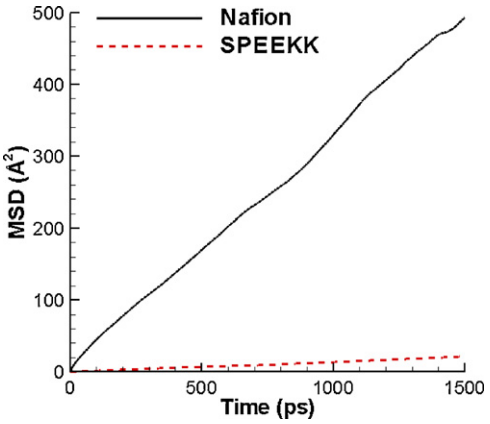

Fig. 10. MSDs of methanol permeability in Nafion and SPEEKK membranes at 300 K.

Table 5
Comparison of diffusion coefficient of methanol molecules in the Nafion and the SPEEKK between simulation results and similar experiments [8,27].

Diffusion coefficient ($cm^2\ s^{-1}$) of methanol molecules	Membrane	
	Nafion	SPEEKK
MD prediction	0.55×10^{-5}	0.024×10^{-5}
Experiment	0.50×10^{-5}	0.017×10^{-5}

3.5. Methanol permeability analysis

Methanol permeation through the membrane deteriorates the performance of DMFCs significantly. This can be analyzed from the MD simulation results. Fig. 10 shows the MSDs of methanol molecules for the Nafion and the SPEEKK membranes. The slope of the MSD trace in the Nafion shows much steeper than in the SPEEKK; implying that the methanol permeation will be more serious in the Nafion membrane. Table 5 shows the comparison of methanol diffusion coefficients in the Nafion and in the SPEEKK between our simulation and experiments [8,27]. They are in reasonable agreement. The diffusion coefficient of methanol in the SPEEKK is much lower than that in the Nafion. A rationalization of this result is attributed to (a) the sulfonic-acid groups are dispersed throughout the SPEEKK membrane; (b) the phase separation in the SPEEKK is less significant; and (c) the water transport channels in SPEEKK are narrower compared with those in the Nafion. We can draw a conclusion here that methanol molecules travel with water molecules and hydronium ions via the hydrophilic sulfonic-acid groups. Narrower water channels in the SPEEKK make the methanol diffusion coefficient in the SPEEKK much lower than that in the Nafion. The results indicate that the SPEEKK membrane is able to reduce the methanol permeability from the Nafion membrane without much sacrifice of water and hydronium diffusion in DMFCs.

4. Conclusions

The molecular structure and transport dynamics of hydrated Nafion and SPEEKK membranes are investigated in this paper by means of molecular simulation techniques. It is found that both hydrated Nafion and SPEEKK membranes form the phase separation of hydrophobic and hydrophilic regions; the hydrated SPEEKK forms less phase separations in comparison with the Nafion. Narrower and more branched water channels in the SPEEKK result in a larger interface between the hydrophobic and hydrophilic regions. These characteristics lead to a rise in the number of water clusters and a decrease of water molecule number in each cluster in the SPEEKK membrane. Narrower water channels in the SPEEKK make the methanol diffusion coefficient in the SPEEKK much lower than that in the Nafion. The results indicate that the SPEEKK membrane is able to reduce the methanol permeability from the Nafion membrane without much sacrifice of water and hydronium diffusion in DMFCs. This paper has established a molecular simulation technique to investigate the nano-technology to further improve the methanol permeation problem in DMFCs by means of designing new molecular structure in proton-conducting electrolytic membranes. This simulation technique is an effective and efficient way to help designing new materials in the future.

Acknowledgements

National Science Council supported this work under contract number: NSC 97-ET-7-007-007 and NSC 97-2212-E-007-059. We are grateful to the National Center for High-performance Computing for providing computing facilities.

References

[1] USDOE, Fuel Cell Handbook, 7th ed., EG&G Technical Services, Morgantown, 2004 (Chapter 3).
[2] A. Carbone, R. Pedicini, G. Portale, A. Longo, L. D'Ilario, E. Passalacqua, J. Power Sources 163 (2006) 18–26.
[3] X. Li, C. Zhao, H. Lu, Z. Wang, H. Na, Polymer 46 (2005) 5820–5827.
[4] X. Li, D. Chen, D. Xu, C. Zhao, Z. Wang, H. Lu, H. Na, J. Membr. Sci. 275 (2006) 134–140.
[5] X. Li, X. Hao, D. Xu, G. Zhang, S. Zhang, H. Na, D. Wang, J. Membr. Sci. 281 (2006) 1–6.
[6] M. Ise, K.D. Kreuer, J. Maier, Solid State Ionics 125 (1999) 213–223.
[7] R. Jiang, H.R. Kunz, J.M. Fenton, J. Power Sources 150 (2005) 120–128.
[8] X. Li, C. Liu, H. Lu, C. Zhao, Z. Wang, W. Xing, H. Na, J. Membr. Sci. 255 (2005) 149–155.
[9] X. Li, G. Zhang, D. Xu, C. Zhao, H. Na, J. Power Sources 165 (2007) 701–707.
[10] S.J. Paddison, J. New Mater. Electrochem. Syst. 4 (2001) 197–207.
[11] S.J. Paddison, R. Paul, K.D. Kreuer, Phys. Chem. Chem. Phys. 4 (2002) 1151–1157.
[12] C.H. Cheng, P.Y. Chen, C.W. Hong, J. Electrochem. Soc. 155 (2008) B435–B442.
[13] P.Y. Chen, C.P. Chiu, C.W. Hong, J. Electrochem. Soc. 155 (2008) B1255–B1263.
[14] Hypercube Inc, HyperChem Reference Manual, 2002 (Chapter 8).
[15] N. Agmon, Chem. Phys. Lett. 244 (1995) 456–462.
[16] S.L. Mayo, B.D. Olfason, W.A. Goddard, J. Phys. Chem. 94 (1990) 8897–8909.
[17] W.L. Jorgensen, J. Phys. Chem. 90 (1986) 1276–1284.
[18] W.L. Jorgensen, D.S. Maxwell, J. Tirado-Rives, J. Am. Chem. Soc. 118 (1996) 11225–11236.
[19] H.J.C. Berendsen, J.R. Grigera, T.P. Straatsma, J. Phys. Chem. 91 (1987) 6269–6271.
[20] A. Burykin, A. Warshel, Biophys. J. 85 (2003) 3696–3706.
[21] W. Smith, M. Leslie, T.R. Forester, The DLPoly_2 User Manual, CCLRC, Daresbury Laboratory, 2003.
[22] L. Verlet, Phys. Rev. 159 (1967) 98–103.
[23] J.P. Ryckaert, G. Ciccotti, H.J.C. Berendsen, J. Comput. Phys. 23 (1977) 327–341.
[24] M.P. Allen, D.J. Tildesley, Computer Simulation of Liquids, Oxford University Press, New York, 1987 (Chapter 5).
[25] K.D. Kreuer, J. Membr. Sci. 185 (2001) 29–39.
[26] T.A. Zawodzinski, M. Neeman, L.O. Sillerud, S. Gottesfeld, J. Phys. Chem. 95 (1991) 6040–6044.
[27] X. Ren, T.E. Springer, T.A. Zawodzinski, S. Gottesfeld, J. Electrochem. Soc. 147 (2000) 466–474.